ELSEVIER

Journal of Photochemistry and Photobiology
A: Chemistry 88 (1995) 169–178

Journal of PHOTOCHEMISTRY AND PHOTOBIOLOGY A: CHEMISTRY

Heterogeneous photocatalytic oxidation of dilute toluene–chlorocarbon mixtures in air

Michael L. Sauer, Michael A. Hale, David F. Ollis

Department of Chemical Engineering, North Carolina State University, Raleigh, NC 27695-7905, USA

Received 2 December 1994; accepted 26 January 1995

Abstract

At 1–2 ms residence time, the photocatalytic oxidation of dilute (10–750 mg m^{-3}) mixtures of toluene and 1,1,3-trichloropropene (TCP) or perchloroethylene (PCE) in air increased the toluene conversion to 100% from the pseudo-steady single-component toluene feed levels of 10%–20%. A chain mechanism involving chlorine radical attack of the toluene and halogenate, previously proposed by Luo and Ollis (*J. Catal., 00* (1994) 00–00) for toluene–trichloroethylene mixtures, is extended to rationalize the current results. The conversion enhancement occurred at low toluene concentrations (up to 22 mg m^{-3}) and high TCP/PCE levels. Increasing the toluene concentration to 43 mg m^{-3} completely quenched the TCP oxidation chain mechanism, giving the same toluene conversion as observed for the toluene-only feeds. The possible enhancement of toluene conversion in toluene–halomethane (methylene chloride, chloroform, carbon tetrachloride) mixed feeds was examined. Carbon tetrachloride and chloroform were ineffective as toluene promoters, and were not photo-oxidized themselves, either alone or in mixtures. Methylene chloride photo-oxidation occurred at very modest rates and conversion, and toluene–methylene chloride mixtures exhibited only a slight enhancement of toluene conversion. Catalyst deactivation was observed with all toluene feeds. Both chlorocarbon addition (TCP, PCE) and humidification slowed, but did not eliminate, deactivation.

Keywords: Photocatalytic oxidation; Toluene; Perchloroethylene; Trichloropropene

1. Introduction

Gas–solid heterogeneous photocatalytic oxidation of single-compound feeds has been previously demonstrated for alkanes [1–6], alcohols [7–12], aldehydes [12–14], ketones (acetone) [12,15,16], aromatics (toluene [13,17], *m*-xylene [12,14]), halogenates (trichloroethylene [18–29]) and inorganics (ammonia [30]). Photocatalysis is thus established as having potential air treatment and purification technology because of its broad applicability to common, oxidizable air contaminants.

The commercialization prospects for photocatalytic air treatment have recently been discussed by Miller and Fox [31], who estimated the capital and operating costs for treatment of four examples of contaminated air streams: soil vapor extract (100 ppm trichloroethylene (TCE)), air stripper vent (50 ppm benzene, 250 ppm other VOC), product dryer vent (including 25 ppm methanol, 25 ppm ethanol) and a paint drying vent (10 ppm xylene, odors, plasticizers, surfactants). They concluded that only the TCE and methanol/ethanol examples were cost competitive and that, "Photocatalysis research should focus on improvements in catalyst performance .... for other compounds to expand the market for the technology".

As TCE, methanol and ethanol are among the very few individual compounds exhibiting 80%–100% quantum efficiencies in photocatalyzed oxidation, the Miller–Fox [31] challenge is clearly to raise the quantum efficiencies and move conversions for other reactants up to 80%–100%. For example, while aromatics (benzene (B), toluene (T) and xylene (X)) and oxygenated solvents (e.g. acetone) are convertible photocatalytically, their respective single-contaminant quantum efficiencies for disappearance are modest (10%–15% for T (this work), 1%–2% for acetone [12].

Enhanced photocatalyzed reaction rates have been observed by Berman and Dong [32] when TCE was added to air lightly contaminated with iso-octane, methylene chloride or chloroform. Luo and Ollis [33] have extended this halide enhancement observation to demonstrate TCE-enhanced conversions for T oxidation which equal 100%. The present paper explores the ability of other chlorocarbons to enhance T quantum yields and conversions to the 80%–100% range of commercial interest.

Elsevier Science S.A.
SSDI 1010-6030(95)04052-8

1.1. Toluene (T)

Ibusuki and Takeuchi [17] studied the gas–solid photocatalyzed oxidation of T at 10 min residence times in a batch reactor. They identified trace benzaldehyde as the only gas phase intermediate and demonstrated a nearly stoichiometric formation of carbon dioxide. Feed water vapor increased the carbon dioxide yield and decreased benzaldehyde formation; low T conversion was observed in the absence of feed water vapor.

Luo and Ollis [33] recently examined the gas–solid photocatalytic oxidation of T during 4–5 ms residence times in a single-pass catalyst powder bed. No intermediates were detected by gas chromatography (TC) (flame ionization detector) (FID)) analysis; CO_2 analysis was not performed. They found that the TiO_2 catalyst activity decreased for each run, when the same catalyst was used on consecutive days, until the catalyst was completely deactivated. The completely deactivated catalyst, which had a brown color, was extracted in methanol and analyzed by gas chromatography–mass spectrometry (GC–MS) to identify the adsorbed deactivating species; four peaks were revealed, one of which was benzoic acid.

1.2. Trichloroethylene (TCE)

The photocatalyzed oxidation of TCE was first reported by Dibble and Raupp [18] to be much faster than that of hydrocarbons and oxygenates, and apparent quantum yields exceeding 100% have often been measured for TCE disappearance since 1988. These very high photon efficiencies imply that a chain mechanism is occurring on the TiO_2 surface and researchers have recently examined gas phase chlorine oxidation mechanisms of TCE attack to understand better the potential photocatalyst surface pathways. In particular, while photocatalytic oxidations are frequently assumed to proceed by way of either hydroxyl radical or direct hole (h^+) attack of the contaminant of interest, TCE oxidation in the gas phase can be initiated by chlorine radicals and proceeds through a chain mechanism which generates most of the intermediates (dichloroacetaldehyde chloride (DCAC)) and phosgene (CCl_2O) and the final products (CO_2, HCl) observed during photocatalytic oxidation. This gas phase mechanism is summarized below of its presumed importance in our results.

Initiation

$$Cl_2 + h\nu \longrightarrow 2^{\cdot}Cl \quad (1)$$

Propagation

$$CCl_2CHCl + {}^{\cdot}Cl \longrightarrow CHCl_2CCl^{\cdot}Cl \quad (2)$$

$$CHCl_2CCl^{\cdot}Cl + O_2 \longrightarrow CHCl_2CCl_2O^{\cdot}O \quad (3)$$

$$2CHCl_2CCl_2O^{\cdot}O \longrightarrow 2CHCl_2CCl_2O^{\cdot} + O_2 \quad (4)$$

$$CHCl_2CCl_2O^{\cdot} \longrightarrow CHCl_2CCl(O) + Cl^{\cdot} \quad (5)$$

$$CHCl_2CCl_2O^{\cdot} \longrightarrow CCl_2O + CHCl_2^{\cdot} \quad (6)$$

$$CHCl_2^{\cdot} + \tfrac{1}{2}O_2 \longrightarrow CO + HCl + Cl^{\cdot} \quad (7)$$

$$CHCl_2^{\cdot} + Cl_2 \longrightarrow CHCl_3 + Cl^{\cdot} \quad (8)$$

Termination

$$CHCl_2CClCl^{\cdot} + CHCl_2CClCl^{\cdot} \longrightarrow \text{chain termination} \quad (9)$$

Quantum yields as high as 200% were calculated by Huybrechts and Meyers [34].

1.3. Trichloroethylene and toluene mixed feeds

Although the gas–solid heterogeneous photocatalytic oxidation of TCE has been studied extensively [18–29], these studies have been limited to single-contaminant feeds. A contrasting recent report by Berman and Dong [32] using dual-contaminant feeds found that the addition of appreciable TCE enhanced the individual conversion rates of iso-octane, methylene chloride and chloroform, while the simultaneous TCE conversion was still 100%. They proposed that the added "sensitizer" (TCE) provided the chlorine radicals required to initiate a chain-propagated destruction of the second pollutant; however, no explicit mechanism was proposed.

1.4. Trichloroethylene and toluene mixed feed mechanism

Recently, Luo and Ollis [33] have reported the gas phase heterogeneous photocatalytic oxidation of TCE–T mixtures. They found that, for T concentrations below 100 mg m^{-3}, using TCE levels of 220–760 mg m^{-3}, both T and TCE were 100% converted, whereas T-only air feeds gave only 10%–15% conversion at pseudo-steady state. Increasing the T feed levels above 160 mg m^{-3} led to nearly complete quenching of the TCE reaction, and T conversions fell to the levels seen for single-contaminant feed experiments. The gas phase chlorine-radical-initiated oxidation mechanism for TCE of Huybrechts and Meyers [34], adopted by Nimlos et al. [24] and Jacoby [23] in their recent photocatalysis papers, was modified to include chain transfer to T by chlorine radical attack, thereby entraining T in the $Cl^{\cdot}$ radical mechanism, and thus rationalizing the T conversion enhancement and TCE quenching observed when T feed levels are relatively low and high respectively. Their proposed mechanism, sketched below, includes the observation by Berman and Dong [32] that, in the absence and presence of water, the major chlorine products are Cl_2 and HCl respectively.

Toluene (non-chain sequence)

$$TiO_2 + OH^- + h\nu \longrightarrow {}^{\cdot}OH \quad (10)$$

$$^{\cdot}OH + \phi CH_3 \longrightarrow \phi CH_2^{\cdot} + H_2O \quad (11)$$

$$\phi CH_2^{\cdot} + (O_2, {}^{\cdot}OH) \longrightarrow CO_2 + H_2O \quad (12)$$

TCE (chain). Initiation

$$TiO_2 + TCE + h\nu \longrightarrow Cl^{\cdot} + \ldots \quad (13)$$

Propagation

$$CCl_2CHCl + Cl^{\cdot} \longrightarrow CHCl_2CClCl^{\cdot} \quad (14)$$

$$CHCl_2CClCl^{\cdot} + O_2 \longrightarrow CHCl_2CCl_2OO^{\cdot} \quad (15)$$

$$2CHCl_2CCl_2OO^{\cdot} \longrightarrow 2CHCl_2CCl_2O^{\cdot} + O_2 \quad (16)$$

$$CHCl_2CCl_2O^{\cdot} \longrightarrow CHCl_2CCl(O) + Cl^{\cdot} \quad (17)$$

Termination

$$2Cl^{\cdot} \longrightarrow Cl_2 \text{(water absent)} \quad (18)$$

$$Cl^{\cdot} + \ldots \longrightarrow \ldots + HCl \text{(water present)} \quad (19)$$

Chain transfer

$$Cl^{\cdot} + \phi CH_3 \longrightarrow \phi CH_2^{\cdot} + HCl \quad (20)$$

(also abstraction of ring hydrogen is possible)

1.5. Catalyst activation/deactivation

The commercial potential of any catalyst depends not only on its initial activity, but also its expected lifetime in use; hence catalyst deactivation studies are important to ascertain the rate of the latter and to discover strategies to decrease deactivation or allow regeneration.

During the photocatalytic oxidation of TCE over TiO_2, an initial activation period of 60–80 min was noted by Phillips and Raupp [22]. During this interval, the photodesorption of water and the photodriven consumption of surface hydroxyl groups were measured. Luo and Ollis [33] found similar activation periods for TCE oxidation.

Catalyst deactivation has been observed for TCE-containing air feeds. In the absence of feed water vapor, TCE photocatalyzed oxidation decreases rapidly, presumably due to exhaustion of surface hydroxyls (Dibble and Raupp). Larson and Falconer [29] used temperature-programmed desorption to characterize CO and CO_2 coverages on fresh, used and deactivated TiO_2 photocatalysts following TCE photocatalyzed oxidation. The total desorbed quantities of $(CO + CO_2)$ μmol (g $TiO_2)^{-1}$ were 56, 359 and 910 for the respective catalysts; the last number is similar to the 830 μmol total surface sites (g $TiO_2)^{-1}$ estimated assuming 10^{15} sites cm^{-2}. Thus a deactivated catalyst appears to be fully blocked by strongly adsorbed oxycarbon species. Earlier IR studies of the photocatalytic oxidation of 1-butanol by Blake and Griffin [11] indicated the formation of carbonate species and concurrent catalyst deactivation.

Luo and Ollis [33] noted photocatalyst deactivation with T–TCE–air feeds; the deactivation rate increased monotonically as the T level was increased from 88 to 150 mg m^{-3}. Thus water vapor, oxygen–carbon species and, potentially, chlorine-containing adsorbates all play a role in the as yet incompletely understood deactivation mechanism(s).

2. Method

The photoreactor was a downflow single-pass titanium dioxide powder bed with near-UV illumination, used previously [12,33]. The photoreactor was cylindrical (4 cm high, 2 cm in diameter) with an internal fritted disk, onto which the TiO_2 powder layer was placed. The contaminated air stream was passed downward through the powder layer and fritted glass disk at a flow rate of 0.96 cm^3 s^{-1} and a residence time of 1.5 ms in the illuminated portion of the powder layer. A quartz plate at the top allowed illumination from above the photocatalyst layer.

The catalyst powder used without pretreatment was Degussa P25 titanium dioxide, which is mostly anatase, with a primary particle diameter of 30 nm and a specific surface area of 50 ± 15 m^2 g^{-1} (Degussa). The P25 particles were spherical and non-porous, with a stated purity of better than 99.5% TiO_2 (Degussa). Stated impurities include Al_2O_3 (<0.3%), HCl (<0.3%), SiO_2 (<0.2%) and Fe_2O_3 (<0.01%). The organic chemicals were of high performance liquid chromatography (HPLC) grade, supplied by Fisher and Aldrich. The pressurized gases (air, helium, hydrogen) were scientific grade, supplied by a local vendor.

A typical experiment was started by evacuating a feed gas reservoir (to remove residual contaminants), then filling the reservoir with scientific grade air to atmospheric pressure. The desired amounts of liquid contaminants and water were injected through a sample port into the reservoir, where evaporation occurred; the reservoir was then further pressurized to 2 atm. Mass flow controllers (Linde FM4575) were used to control the parallel feeds from the gas reservoir and compressed air tank. The use of dual feeds, from the separate contaminated air reservoir and the pure tank air, allowed the contaminant feed concentration to the reactor to be varied easily by changing the mass flow controller settings, and allowed longer run times by using lower reservoir flow rates. Next, the contaminated air was passed through the dark reactor until the inlet and outlet contaminant concentrations were equal (usually 60–120 min), indicating that the contaminant had reached adsorption/desorption equilibration with the TiO_2 powder layer. The illumination source (Blak-Ray 100 W medium pressure UV lamp with a near-UV

filter attachment) was then turned on and the outlet contaminant concentration was monitored until either the outlet reached a pseudo-steady state or the gas reservoir dropped to 1 psig (approximately 6 h). All air samples were analyzed by GC (Perkin–Elmer Sigma Series 1) operating with an FID and an SS Alltech column with AT-1000 (10%) on 80/100 Chromosorb W-AW packing. The photon generation rate of the lamp, as determined by actinometry, was 8×10^{-5} einsteins min^{-1}.

3. Results

To determine whether chlorinated hydrocarbons other than the previously noted TCE can be used to enhance the photocatalyzed conversion of T, we tested 1,1,3-trichloropropene (TCP), perchloroethylene (PCE), methylene chloride (CH_2Cl_2), chloroform ($CHCl_3$) and carbon tetrachloride (CCl_4) addition to T–air mixtures. Results are presented below for air feeds containing the following: (1) T; (2) TCP–T; (3) PCE–T; (4) chloromethane–T. Parent compound disappearance was monitored, and no intermediates were detected on the single column used.

3.1. Toluene

Fig. 1 shows the conversion of T as a function of time, with and without water vapor in the feed. The conversion of T, initially high (approximately 75%) for both cases, declines rapidly at first, then more slowly to 15%–25% (no water vapor) or 0%–10% (water vapor present) in an apparent two-stage process. Water vapor leads to quicker deactivation of the catalyst, providing total activity loss at 300 min, whereas T conversion in the absence of water is still approximately 15%.

3.2. 1,1,3-Trichloropropene (TCP)

Fig. 2 shows that the TCP conversion is 95%–100% at all times for a feed of 219 mg m^{-3} TCP and 492 mg m^{-3} water. The apparent quantum yield (molecules TCP converted per number of photons received) is 150%, indicating that a chain mechanism is occurring.

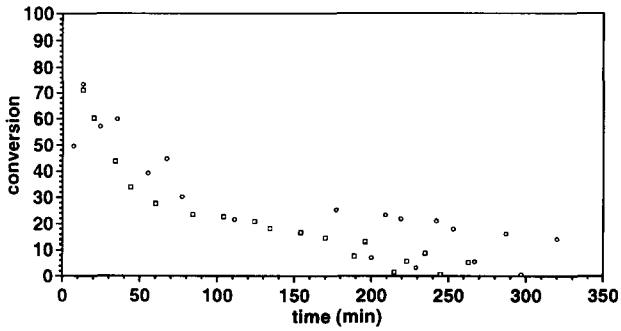

Fig. 1. Toluene conversion vs. time (T_0=26 mg m^{-3}): water vapor, 0 mg m^{-3} (○) or 492 mg m^{-3} (□).

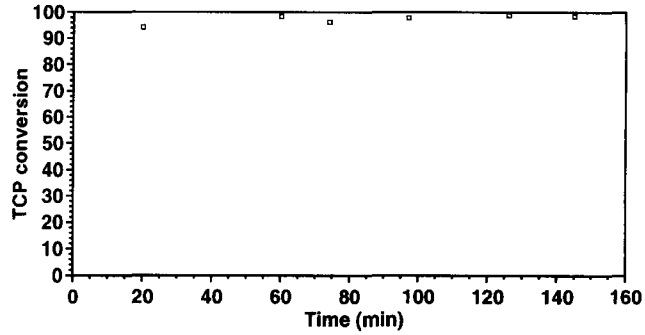

Fig. 2. Trichloropropene conversion vs. time (TCP_0=219 mg m^{-3}; water vapor, 492 mg m^{-3}).

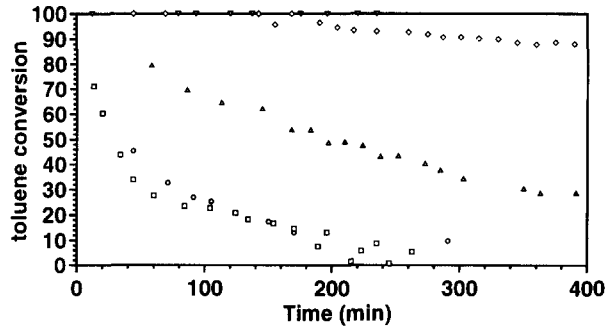

Fig. 3. Enhancement of toluene conversion and reduction of catalyst deactivation by TCP presence: (□) T_0=26 mg m^{-3}, TCP_0=0 mg m^{-3}; (○) T_0=43 mg m^{-3}, TCP_0=219 mg m^{-3}; (△) T_0=22 mg m^{-3}, TCP_0=317 mg m^{-3}; (◇) T_0=10 mg m^{-3}, TCP_0=333 mg m^{-3}; (▽) T_0=10 mg m^{-3}, TCP_0=305 mg m^{-3}. H_2O=492 mg m^{-3} (all cases).

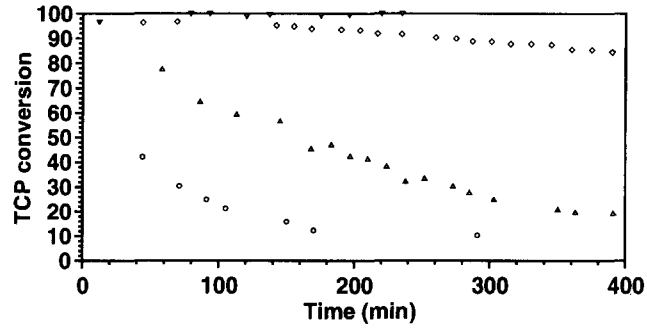

Fig. 4. Depression of TCP conversion (vs. Fig. 2) and increased catalyst deactivation rate by presence of toluene (same symbols as in Fig. 3).

The conversion of T vs. time for different feed mixtures of T and TCP in lightly humidified air is shown in Fig. 3. Decreasing T feed concentrations lead to both a strong enhancement of T conversion (up to 100% for a T feed of 10 mg m^{-3}) and markedly slower deactivation. The corresponding TCP conversion data vs. time (Fig. 4) show a similar behavior, with TCP conversion also increasing to nearly 100% at the lower T feed levels of 22 and 10 mg m^{-3}.

Fig. 5 displays the conversion of T vs. TCP for the same T–TCP feed mixtures as shown in Figs. 3 and 4. The conversions decrease together from approximately 100% in a nearly linear fashion. The number of catalyst monolayer equivalents (meq.) converted for T vs. TCP is shown in Fig. 6 (see Appendix for meq. calculation). The conversion selectivity for the mixture is given by the meq. ratio of TCP to T and has constant values of approximately 3, 9 and 20 for toluene feed levels of 43, 22 and 10 mg m^{-3} respectively.

The deactivation of the titanium dioxide catalyst over 6 h runs during each day of a 4 day period is shown for a T (□)–TCP(○) mixed feed in Fig. 7. There is some variation in the fresh feed mixtures over the 4 days (T mg m^{-3}): day 1 = 20.3, day 2 = 24.7, day 3 = 19.4 and day 4 = 21.1; TCP (mg m^{-3}): day 1 = 331, day 2 = 380, day 3 = 323 and day 4 = 335). After an initial activation of the catalyst in the first half hour of day 1, conversion of both species decreases steadily over days 1 and 2. The catalyst recovers activity at the start of day 3 (the T and TCP feed concentrations are decreased from day 2 levels) and is then deactivated continuously for days 3 and 4. As the gas reservoir is large enough for approximately 6 h runs, a new mixture is prepared each day and fed to the illuminated catalyst. At the end of each run (day), the catalyst bed is left in the dark overnight with no gas flow. The 4 day deactivation experiment is presented in Fig. 8 as meq.

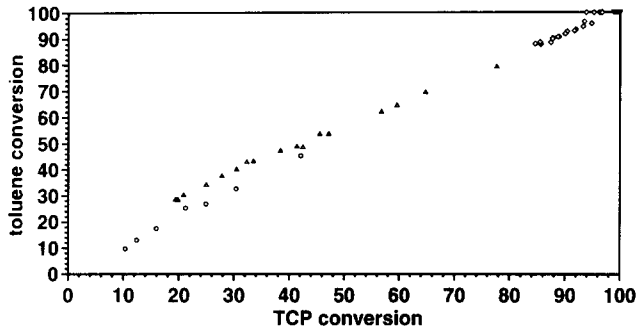

Fig. 5. Trajectory of toluene vs. TCP conversion on deactivating catalyst (same symbols as in Fig. 3).

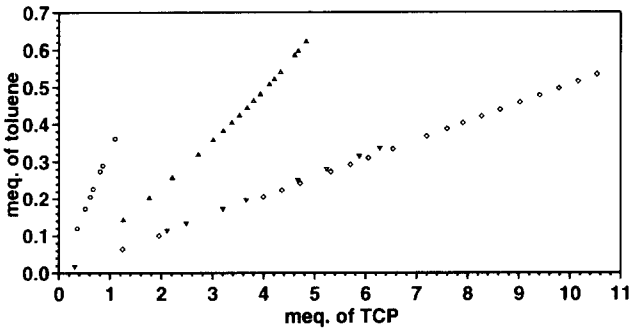

Fig. 6. Cumulative monolayer equivalents converted of toluene vs. TCP (same symbols as in Fig. 3).

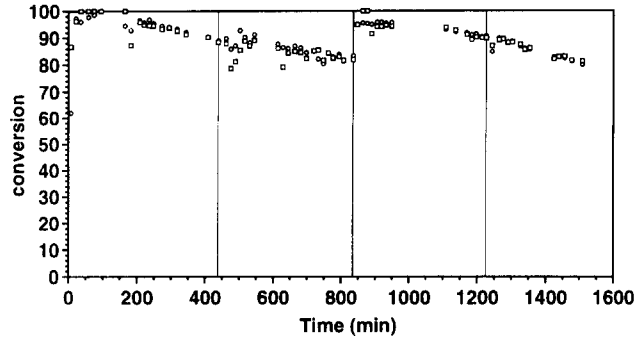

Fig. 7. Catalyst deactivation over successive 6 h runs (one per day) (T (□), TCP (○)). Initial conditions: day 1 (T_0 = 20.3 mg m^{-3}, TCP_0 = 331 mg m^{-3}), day 2 (T_0 = 24.7 mg m^{-3}, TCP_0 = 380 mg m^{-3}), day 3 (T_0 = 19.4 mg m^{-3}, TCP_0 = 323 mg m^{-3}) and day 4 (T_0 = 21.1 mg m^{-3}, TCP_0 = 335 mg m^{-3}).

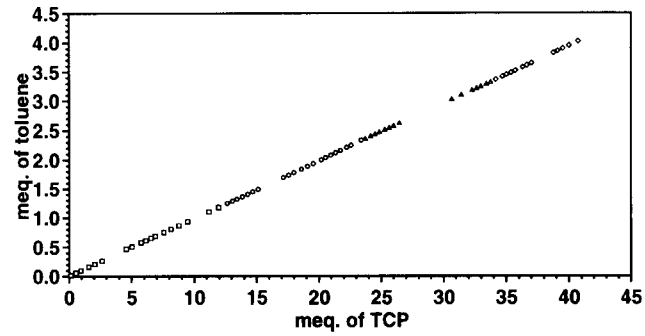

Fig. 8. Cumulative monolayer equivalents converted of toluene vs. TCP (day: 1 (□), 2 (○), 3 (△) and 4 (◇)).

of T converted vs. meq. of TCP converted. The selectivity of TCP to T is approximately ten for all 4 days, close to the selectivity of nine noted earlier for similar T and TCP levels.

3.3. Perchloroethylene (PCE)

With PCE–air feeds, the catalyst activity increases rapidly from a PCE conversion of 14% initially to 75% after 50 min (data not shown). The conversion then increases slowly to 85% after 300 min and appears to be still rising at the time of reservoir pressure exhaustion. Feed water vapor presence has no effect on PCE initial conversion (but influences the deactivation rate, discussed below). The apparent quantum yield for PCE (at 85% conversion) is 260%, indicating that a chain mechanism is occurring.

Fig. 9 presents the conversion of T and PCE vs. time for a feed mixture of 40 mg m^{-3}, 740 mg m^{-3} PCE and 492 mg m^{-3} water. PCE conversion decreases steadily throughout the run, from an initial value of 80% to 0% at 300 min. T is completely converted for 250 min; when the PCE conversion falls to about 13%, the T conversion drops sharply, and when the PCE conversion activity reaches zero, the T conversion reaches the 10%–25% range characteristic of T-only

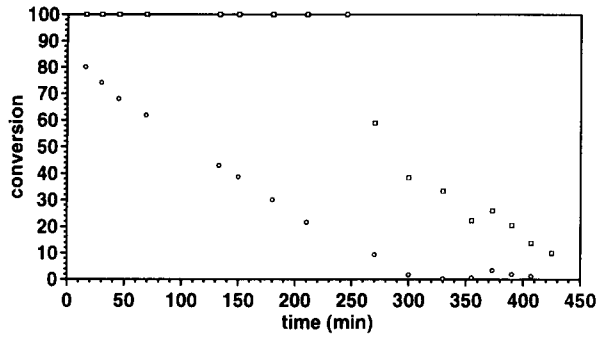

Fig. 9. Toluene (□) and PCE (○) conversion vs. time: $T_0 = 40$ mg m^{-3}; $PCE_0 = 740$ mg m^{-3}; $H_2O = 492$ mg m^{-3}.

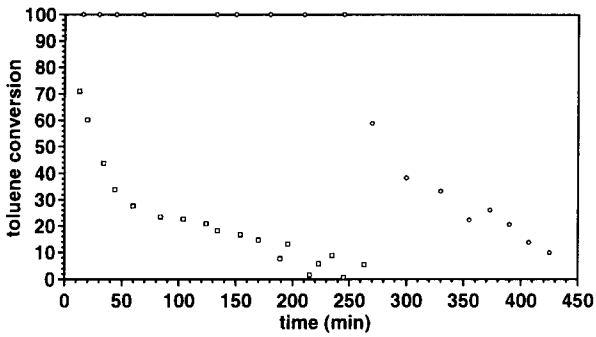

Fig. 10. Enhanced toluene conversion and delayed catalyst deactivation by PCE presence: (□) $T_0 = 26$ mg m^{-3}, $PCE_0 = 0$ mg m^{-3}; (○) $T_0 = 40$ mg m^{-3}, $PCE_0 = 740$ mg m^{-3}. $H_2O = 492$ mg m^{-3} (both cases).

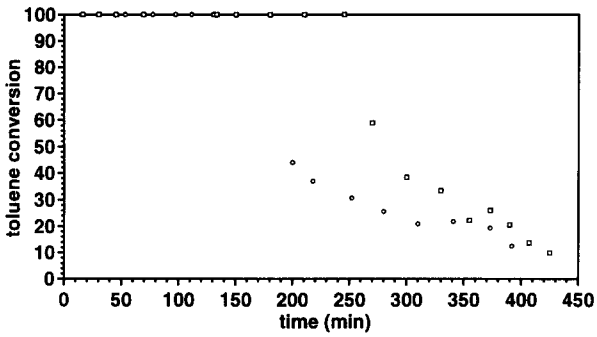

Fig. 11. Influence of water vapor on toluene conversion and deactivation ($PCE_0 = 740$ mg m^{-3} always; (□) $T_0 = 40$ mg m^{-3}, $H_2O = 492$ mg m^{-3}; (○) $T_0 = 33$ mg m^{-3}, $H_2O = 0$ mg m^{-3}).

feeds. A comparison of T conversion vs. time for the T-only vs. mixed T–PCE cases (Fig. 10) shows that PCE promotion yields 100% T conversion for 250 min vs. a rapid deactivation for T only; beyond 250 min, the T–PCE deactivation profile is very similar to that for T-only feeds.

In the absence of feed water vapor, PCE enhancement of T conversion is again observed. T conversions are now 100% for only 130 min (Fig. 11) (vs. 250 min in the presence of water vapor (Fig. 10)), after which the conversion drops sharply when the PCE conversion falls to less than 10%.

The influence of water vapor on T and PCE conversions in a T–PCE feed mixture is indicated in Figs. 11 and 12 respectively. The T and PCE conversions both decrease more quickly in the absence of water, until at longer times there is no conversion of PCE with or without feed water vapor, and T conversions reach the 10%–15% range characteristic of T-only air feeds.

Fig. 13 shows T vs. PCE conversion for T–PCE–water(no water) feed mixtures. The T conversion remains at 100% while the PCE conversion declines to 10%; it then decreases sharply from 100% to 13% for a corresponding PCE conversion decrease of 10% to 0% (no water feed) or 20% to 0% (water feed). Fig. 14 plots the cumulative meq. of T vs. meq. of PCE

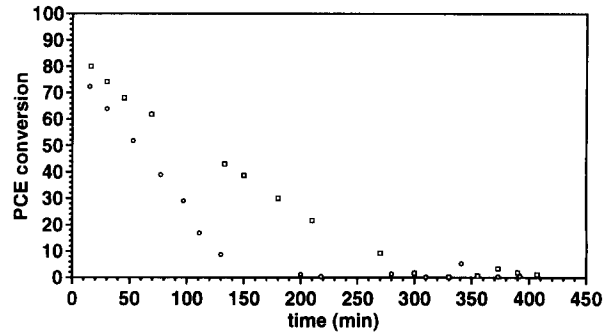

Fig. 12. Influence of water vapor on PCE conversion (same symbols as in Fig. 11).

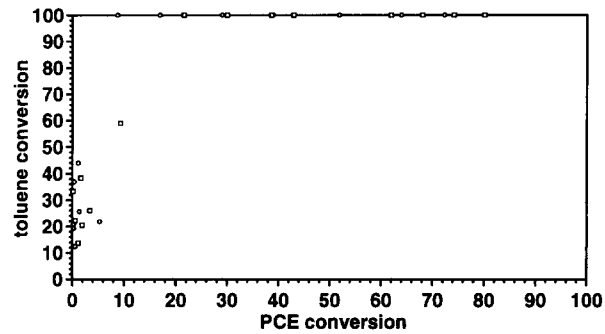

Fig. 13. Trajectory of toluene vs. PCE conversion on deactivating catalyst (same symbols as in Fig. 11).

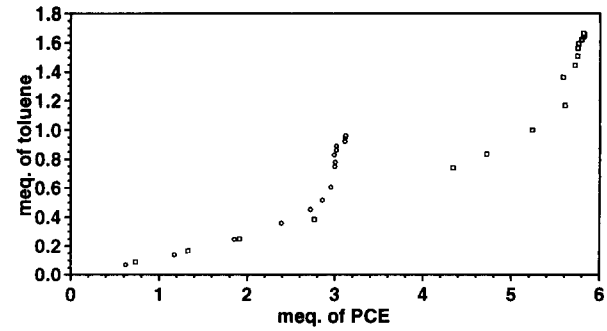

Fig. 14. Cumulative monolayer equivalents converted of toluene vs. PCE (same symbols as in Fig. 11).

converted for the same feed mixtures. Both reactants are converted to some degree until approximately 1 meq. T (0.5 mg T for water-free feed) has been converted, followed by total quenching of the PCE reaction.

3.4. Chloromethanes

Methylene chloride enhances the T conversion slightly (approximately 5%) in the presence of water vapor at all times, while chloroform and carbon tetrachloride have no influence. Correspondingly, methylene chloride is converted (4% or less) at a modest rate, and chloroform and carbon tetrachloride are unreactive in the presence of T. In the absence of feed water vapor, T conversion is not enhanced by any of these halomethanes.

4. Discussion

4.1. Chloro-olefin chain mechanism

A non-chain mechanism was presented by Kleindienst et al. [35] for the homogeneous gas phase attack of TCE by hydroxyl radicals which leads to the formation of chlorine radicals. TCE reacts with hydroxyl radicals forming a radical intermediate, which is rapidly converted in several steps to a chloroethoxy radical and a chlorine radical

$$CCl_2CHCl + {}^{\cdot}OH \longrightarrow {}^{\cdot}CCl_2CHClOH \quad (21)$$

$$^{\cdot}CCl_2CHClOH + O_2 \longrightarrow {}^{\cdot}OOCCl_2CHClOH \quad (22)$$

$$2{}^{\cdot}OOCCl_2CHClOH \longrightarrow 2{}^{\cdot}OCCl_2CHClOH + O_2 \quad (23)$$

$$^{\cdot}OCCl_2CHClOH \longrightarrow CHClOHCCl(O) + Cl^{\cdot} \quad (24)$$

For photocatalytic TCE oxidation, Jacoby [23] proposed a mechanism combining aspects of the Kleindienst et al. [35] and Huybrechts–Meyers [34] mechanisms. Anpo et al. [36] showed that, on exposure to near-UV irradiation, hydroxy radicals are produced on the surface of TiO_2 in the presence of adsorbed water vapor. Thus the Kleindienst et al. [35] mechanism could occur on a TiO_2 surface, and replace Cl_2 photolysis as the initiation step which provides chlorine radicals. The Huybrechts–Meyers [34] mechanism could then follow on the TiO_2 surface. Jacoby [23] also proposed a likely route for the heterogeneous photocatalyzed destruction of the DCAC intermediate, leading to the formation of a second observed intermediate, phosgene (CCl_2O)

$$CHCl_2CCl(O) + {}^{\cdot}OH \longrightarrow {}^{\cdot}CCl_2CCl(O) \quad (25)$$

$$^{\cdot}CCl_2CCl(O) + O_2 \longrightarrow {}^{\cdot}OOCCl_2CCl(O) \quad (26)$$

$$2{}^{\cdot}OOCCl_2CCl(O) \longrightarrow 2{}^{\cdot}OCCl_2CCl(O) + O_2 \quad (27)$$

$$^{\cdot}OCCl_2CCl(O) \longrightarrow CCl_2O + CClO^{\cdot} \quad (28)$$

$$CClO^{\cdot} \longrightarrow Cl^{\cdot} + CO \quad (29)$$

Jacoby [23] performed further experiments on TCE photocatalytic heterogeneous degradation in air to test the proposed mechanism; he identified several products using gas phase Fourier transform IR (FTIR) spectroscopy, including DCAC, $COCl_2$ (phosgene), CO_2, CO and HCl. Nimlos et al. [24] were also able to identify Cl_2 together with the above product mix using a molecular beam mass spectrometer (MBMS) operated in direct sampling mode from the same thin film annular photoreactors as Jacoby [23].

Jacoby [23] found that feeding DCAC to the reactor in the presence of near-UV light and TiO_2 led to the same product mix as observed for a TCE feed, except that Cl_2 was not seen by the MBMS. He also noted that DCAC was not converted in the absence of near-UV light or catalyst.

Two pathways were proposed by Nimlos et al. [24] for TCE photocatalyzed destruction: pathway A, which proceeds through a DCAC intermediate, and pathway B, which yields direct oxidation of TCE to products.

Pathway A

$$2CCl_2CHCl + O_2 \longrightarrow 2CHClOHCCl(O) \quad (30)$$

$$2CHClOHCCl(O) + 2O_2 \longrightarrow 2CO_2 + CO + CCl_2O + 2HCl + Cl_2 \quad (31)$$

$$3CHClOHCCl(O) + WO_2 + XH_2O \longrightarrow 4CO_2 - CO + CCl_2O + YHCl + Z(Cl_2) \quad (32)$$

Pathway B

$$CCl_2CHCl + \tfrac{3}{2}O_2 \longrightarrow CCl_2O + CO_2 + HCl \quad (33)$$

Jacoby [23] found experimentally that up to 85% of TCE was converted to DCAC, and thus pathway A was dominant. DCAC destruction gave different product mixes for dry and wet air feeds. The dry feed (second step, pathway A) yields two CO_2 molecules for each CO (or CCl_2O) molecule, while the wet feed (third step, pathway A) provides four CO_2 molecules for each CO (or CCl_2O) molecule. Quantum yields greater than unity were not observed for DCAC, while TCE gave quantum yields greater than unity, consistent with the chain mechanism with $Cl^{\cdot}$ but not $OH^{\cdot}$. The overall conversion of TCE generated about two CO_2 molecules and two CCl_2O molecules for each CO molecule, which differs from the DCAC case above, thus giving evidence that some direct oxidation of TCE (pathway B) also occurs.

Berman and Dong [32] reported that TCE conversion at longer contact times in the absence or presence of water vapor gave almost exclusively either Cl_2 or HCl respectively, as well as phosgene.

Quantum yields greater than unity for chloro-olefins presumably occur due to the presence of a chain

mechanism. The Cl˙ chain mechanism of Huybrechts–Meyers [34] is consistent with our results, but not conclusively shown, and thus we must consider other plausible enhancement arguments in addition to the above discussion. Bickley and Jayanty [37] reported that UV illumination of hydrated TiO_2 in air leads to the formation of a surface-adsorbed oxygen atom

$$TiO_2 + h\nu \longrightarrow h^+ + e^- \quad (34)$$

$$OH^- + h^+ \longrightarrow {}^{\cdot}OH \quad (35)$$

$$O_2^{ads} + e^- \longrightarrow O_2^{ads-} \quad (36)$$

$${}^{\cdot}OH + O_2^{ads-} \longrightarrow HO_2^{\cdot} + O^{ads-} \quad (37)$$

The surface oxygen atom could react with a chloro-olefin in a manner analogous to the series of homogeneous reactions proposed by Sanhueza et al. [38], leading to several products and intermediates, including chlorine radicals, which could then engage in a chain mechanism with the chloro-olefin, as before

$$O^{ads-} + CHClCCl_2 \longrightarrow$$

$$CCl_2O + CH_2Cl^{\cdot} \longrightarrow CO + Cl_2 + CH_2Cl^{\cdot} \quad (38)$$

$$\longrightarrow CHClCCl_2O^{\cdot} \quad (39)$$

$$\longrightarrow CHCl_2CCl(O) \quad (40)$$

$$\longrightarrow CCl_2H^{\cdot} + CClO^{\cdot} \quad (41)$$

The radical intermediates could then react with O_2 or Cl_2, leading to the formation of further chlorine radicals and a chain mechanism again.

Munuera et al. [39] reported that TiO_2 doped with chlorine atoms could evolve singlet oxygen ($^1O_2$) from its surface on exposure to UV illumination. These singlet oxygen species could then react with the chloro-olefin and engage in a chain mechanism, as discussed above, since singlet oxygen is the reactive intermediate in many photo-oxidations [40].

The surface itself may undergo substantial chlorination, and in the limit, the TiO_2 surface could be converted to $TiCl_4$, as noted by Primet et al. [41] on gentle heating of TiO_2 in 100 Torr of CCl_4. Larson and Falconer [29] used X-ray photoelectron spectroscopy (XPS) to show an accumulation of surface chlorine during gas–solid TCE photo-oxidation on TiO_2. They found that the chlorine was present in two chemically different environments: one was determined to be weakly bound $ClCO^{\cdot+}$ (resulting from phosgene), while the other chlorine state was undetermined. Intermediate compounds may occur; Filby et al. [42] demonstrated via XPS that a ZnO surface, after photocatalytic decomposition of CCl_2F_2, displayed Zn binding energies closer to $Zn(ClO_4)_2$ than to ZnO or $ZnCl_2$.

4.2. Toluene single feed

The stoichiometry of the complete mineralization of T can be written as follows

$$C_7H_8 + 9O_2 \longrightarrow 7CO_2 + 4H_2O \quad (42)$$

T conversion is found here to be somewhat inhibited by the presence of 492 mg m^{-3} water vapor. Both Luo and Ollis [33] and Peral and Ollis [12] previously saw activation at low water levels and inhibition at higher water levels. Water levels would be expected to inhibit T conversion by competing for catalyst surface sites; illumination may partially overcome such competition, since Phillips and Raupp [22] noted earlier that illumination led to water desorption from TiO_2, thus allowing adsorption of TCE, which was otherwise not able to adsorb on the fully hydroxylated surface.

4.3. Toluene–halogenate mixed feeds

T conversion was enhanced markedly in the presence of chloro-olefins and only modestly by methylene chloride.

While T oxidation produces water, the total oxidation of TCE and PCE consumes water, and TCP and methylene chloride are neutral with regard to the production or consumption of water during total oxidation.

TCE

$$CCl_2CHCl + \tfrac{3}{2}O_2 + H_2O \longrightarrow 2CO_2 + 3HCl \quad (43)$$

PCE

$$CCl_2CCl_2 + O_2 + 2H_2O \longrightarrow 2CO_2 + 4HCl \quad (44)$$

TCP

$$CCl_2CHCH_2Cl + 3O_2 \longrightarrow 3CO_2 + 3HCl \quad (45)$$

Methylene chloride

$$CH_2Cl_2 + O_2 \longrightarrow CO_2 + 2HCl \quad (46)$$

The mechanism of enhancement of the T by TCP and PCE could follow a chain mechanism analogous to that presented by Luo and Ollis [33] for T–TCE mixtures. This mechanism has an initiation step (involving hole (h^+) or $OH^{\cdot}$ reaction with TCP or PCE) leading to the formation of a chlorine radical, which then reacts with either TCP or PCE in the chain propagation. The enhancement of T conversion by TCP at low T levels and the decrease in TCP and T conversions at higher T levels are consistent with this mechanism. The formation of chlorine radicals could occur through attack of TCP or PCE by either hydroxyl radicals [35] or oxygen atoms [38,39]; the TiO_2 surface could also be partially/completely converted to an active $Ti–O_x–Cl_y$ surface during the brief activation period.

The selectivities of TCP to T were observed to be dependent on the T feed concentration, where de-

creasing T feeds gave increasing TCP to T selectivity (Fig. 6). The selectivity to TCP to T remained constant, with a value of ten, over a 4 day experiment using a T–TCP (10:305–333) mixed feed. The conversion of T and TCP varied from 100% to 80%, but did not affect the selectivity. In marked contrast, the PCE to T selectivity decreased with time, reaching zero when PCE quenching occurred. These results suggest that PCE is converted only by a chain mechanism (and can thus be completely quenched), whereas TCP can be converted by both a chain mechanism as well as the hydroxyl attack mechanism operating with T-only feeds.

The halomethanes have no carbon–carbon double bond for chlorine radicals to attack in a chain addition mechanism, unlike TCE, TCP and PCE. While a chain mechanism involving chlorine radical attack of T and the chloromethane may occur, no catalyst surface or detailed kinetic studies have been performed to analyze the intermediates and/or products resulting from this proposed mechanism, nor is a chain mechanism required since the quantum efficiency is much smaller than unity in this case. We can only state that the T conversion was enhanced slightly in T–methylene chloride mixtures, and that chloroform and carbon tetrachloride were ineffective as enhancing agents or reactants.

5. Conclusions

The photocatalytic oxidation of T–TCP mixtures in air increased the T conversion to 100% vs. the single-feed "pseudo-steady" level of 10%–20%. A TCE chain photo-oxidation mechanism involving chlorine radical attack of T (by chain transfer) was previously proposed by Luo and Ollis [33] to rationalize such chlorine rate enhancement, and is found to be potentially applicable here also. The TCP enhancement occurred at low T (10–40 mg m^{-3}) and high TCP (219–333 mg m^{-3}) concentrations. Increasing the T level from 10 to 22 mg m^{-3} at a fixed TCP level (320 mg m^{-3}) in a mixed feed led to a decrease in the enhancement of both T and TCP, presumably due to the scavenging of chlorine radicals by T. A further increase in the T feed concentration to 43 mg m^{-3} completely quenched the presumed chain mechanism for TCP oxidation, and decreased the T conversion to levels found for single-contaminant feeds. T–PCE mixtures gave an initial enhancement of T conversion to 100% both with and without feed water vapor; with time the PCE conversion decreased steadily from an initial conversion of approximately 70%–80%; when the PCE conversion fell to 10%–15%, the T conversion declined precipitously from 100% and approached the T-only levels. The presence of feed water vapor increased the conversions for both T and PCE at all times.

The slight enhancement of T disappearance in T–methylene chloride mixed feeds was noted in parallel with weak (4% or less) methylene chloride conversion. Chloroform and carbon tetrachloride were not converted, nor did their presence enhance T conversion. Feed water vapor slightly inhibited T conversion.

Acknowledgements

This work was supported by a Hoechst-Celanese Kenan Fellowship for Engineering, Science and Technology.

Appendix: Calculation of monolayer equivalents converted

This calculation is required to establish how many molecules of a species have been converted per surface site. First, we estimate the number of illuminated (active) catalyst sites

$$SA_{active} = \pi R^2 \delta \rho_c SA_{BET} \quad (A1)$$

$$N_{sites} = SA_{active} \rho_s \quad (A2)$$

where SA_{active} is the active surface area of the catalyst (cm^2), R is the reactor radius (cm), δ is the depth of the active catalyst layer (cm), ρ_c is the density of the solid catalyst (g cm^{-3}), SA_{BET} is the Brunauer–Emmett–Teller (BET) surface area of the non-porous catalyst particles (m^2 g^{-1}), N_{sites} is the number of surface sites and ρ_s is the density of catalyst sites (sites cm^{-2}).

Next, the number of molecules converted over a time period is calculated

$$N_{converted} = \frac{conv_i C_i Q \Delta t N_A}{MW_i} \quad (A3)$$

where $N_{converted}$ is the number of molecules converted, $conv_i$ is the fractional conversion of reactant i, C_i is the feed concentration of i (mg m^{-3}), Q is the volumetric flow rate (cm^3 s^{-1}), Δt is the time period for calculation (s), N_A is Avogadro's number (6.022×10^{23} molecules mol) and MW_i is the molecular weight of species i (mg $mmol^{-1}$).

Finally, the number of monolayer equivalents of i converted is calculated as

$$meq.i = \frac{N_{converted}}{N_{sites}} \quad (A4)$$

References

[1] M. Formenti, F. Juillet, P. Meriaudeau and S.J. Teichner, *Chem. Technol., 1* (1971) 680–681.

[2] N. Djeghri, M. Formenti, F. Juillet and S.J. Teichner, *Faraday Discuss., Chem. Soc., 58* (1974) 185–193.

[3] J.M. Herrmann, J. Disdier, M.-N. Mozzanega and P. Pichat, *J. Catal., 60* (1979) 369–377.
[4] N. Djeghri and S.J. Teichner, *J. Catal., 62* (1980) 99–106.
[5] S.J. Teichner and M. Formenti, in *Photoelectrochemistry, Photocatalysis and Photoreactors,* D. Reidel, 1985, pp. 457–489.
[6] M. Gratzel, K.R. Thampi and J. Kiwi, *J. Phys. Chem., 93* (1989) 4128–4132.
[7] R.I. Bickley, G. Munuera and F.S. Stone, *J. Catal., 31* (1973) 398–407.
[8] A. Walker, M. Formenti, P. Meriaudeau and S.J. Teichner, *J. Catal., 50* (1977) 237–243.
[9] J. Cunnigham and B.K. Hodnett, *J. Chem. Soc., Faraday Trans. 1, 77* (1981) 2777–2801.
[10] P. Pichat, H. Courbon, J. Disdier, M.-N. Mozzanega and J.-M. Herrmann, in *New Horizons in Catalysis,* Elsevier, Amsterdam, 1981, pp. 1498–1499.
[11] N.R. Blake and G.L. Griffin, *J. Phys. Chem., 92* (20) (1988) 5697–5701.
[12] J. Peral and D.F. Ollis, *J. Catal., 136* (1992) 554–565.
[13] K. Suzuki, S. Satoh and T. Yoshida, *Denki Kagaku, 59* (6) (1991) 521–523.
[14] K. Suzuki, in D.F. Ollis and H. Al-Ekabi (eds.), *Proceedings of the First International Conference on TiO_2 Photocatalytic Purification and Treatment of Water and Air, London, Ontario, Canada, 8–13 November, 1992,* Elsevier, 1993, pp. 421–434.
[15] G.B. Raupp and C.T. Junio, *Appl. Surf. Sci., 72* (1993) 321–327.
[16] M.L. Sauer and D.F. Ollis, *J. Catal., 149* (1994) 81–91.
[17] T. Ibusuki and K. Takeuchi, *Atmos. Environ., 20* (9) (1986) 1711–1715.
[18] L.A. Dibble and G.B. Raupp, in *Proceedings of the Arizona Hydrological Society, First Annual Symposium, September 16–17, Phoenix, Arizona, 1988,* 1988, pp. 221–229.
[19] L.A. Dibble, *Ph.D. Thesis,* Arizona State University, 1989.
[20] L.A. Dibble and G.B. Raupp, *Catal. Lett., 4* (1990) 345–354.
[21] L.A. Dibble and G.B. Raupp, *Environ. Sci. Technol., 26* (1992) 492–495.
[22] L.A. Phillips and G.B. Raupp, *J. Mol. Catal., 77* (1992) 297–311.
[23] W.A. Jacoby, *Ph.D. Thesis,* University of Colorado, 1993.
[24] M.R. Nimlos, W.A. Jacoby, D.M. Blake and T.A. Milne, *Environ. Sci. Technol., 27* (1993) 732–740.
[25] M.A. Anderson, S. Yamazaki-Nishida and S. Cervera-March, in D.F. Ollis and H. Al-Ekabi (eds.), *Proceedings of the First International Conference on TiO_2 Photocatalytic Purification and Treatment of Water and Air, London, Ontario, Canada, 8–13 November, 1992,* Elsevier, 1993, pp. 405–420.
[26] W. Holden, A. Marcellino, D. Valic and A.C. Weedon, in D.F. Ollis and H.Al-Ebaki (eds.), *Proceedings of the First International Conference on TiO_2 Photocatalytic Purificaton and Treatment of Water and Air, London, Ontario, Canada, 8–13 November, 1992,* Elsevier, 1993, pp. 393–404.
[27] S. Yamazaki-Nishida, K.J. Nagano, L.A. Phillips, S. Cervera-March and M.A. Anderson, *J. Photochem. Photobiol. A: Chem., 70* (1993) 95–99.
[28] W.A. Jacoby, M.R. Nimlos and D.M. Blake, *Environ. Sci. Technol., 28* (1994) 1661–1668.
[29] S.A. Larson and J.L. Falconer, *Appl. Catal.,* submitted for publication.
[30] H. Mozzanega, J.-M. Herrmann and P. Pichat, *J. Phys. Chem., 83* (1971) (1979) 2251–2255.
[31] R. Miller and R. Fox, in D.F. Ollis and H. Al-Ekabi (eds.), *Proceedings of the First International Conference on TiO_2 Photocatalytic Purification and Treatment of Water and Air, London, Ontario, Canada, 8–13 November, 1992,* Elsevier, 1993, pp. 573–578.
[32] E. Berman and J. Dong, in W.W. Eckenfelder, A.R. Bowers and J.A. Roth (eds.), *The Third International Symposium Chemical Oxidation: Technology for the Nineties, Vanderbilt University, Nashville, Tennessee, 1993,* Technomic Publishing, 1993, pp. 183–189.
[33] Y. Luo and D.F. Ollis, *J. Catal.,* submitted for publication.
[34] G. Huybrechts and L. Meyers, *Trans. Faraday Soc., 62* (1966) 2191–2199.
[35] T.E. Kleindienst, P.B. Shepson, C.M. Nero and J.J. Bufalini, *Inter. J. Chem. Kinet., 21* (1989) 863–884.
[36] M. Anpo, T. Shima and Y. Kubokawa, *Chem. Lett.,* (1985) 1799–1802.
[37] R.I. Bickley and R.K.M. Jayanty, *Discuss. Faraday Soc., 58* (1974) 194–204.
[38] E. Sanhueza, J. Hisatsune and J. Heicklen, *Chem. Rev., 76* (6) (1976) 801–826.
[39] G. Munuera, A. Navio and V. Rives-Arnau, *J. Chem. Soc., Faraday Trans. 1, 77* (1981) 2747–2749.
[40] A.M. Braun, M.-T. Maurette and E. Oliveros, *Photochemical Technology,* Wiley, 1991.
[41] M. Primet, J. Basset and M.V. Mathieu and M. Prettre, *J. Phys. Chem., 74* (15) (1970) 2868–2874.
[42] W.G. Filby, M. Mintas and H. Gusten, Heterogeneous catalytic degradation of chlorofluoromethanes on zinc oxide surfaces, *Ber. Bunsenges Phys. Chem., 85* (1981) 189–192.